Future Trends of Arctic Surface Wind Speeds and their Relationship with Sea Ice in CMIP5 Climate Model Simulations

Stephen Vavrus (sjvavrus@wisc.edu)
University of Wisconsin-Madison https://orcid.org/0000-0002-7612-3109
Ramdane Alkama
JRC: European Commission Joint Research Centre

Research Article

Keywords: Arctic, wind, sea ice, climate change, CMIP, model

Posted Date: June 22nd, 2021

DOI: https://doi.org/10.21203/rs.3.rs-186417/v1

Version of Record: A version of this preprint was published at Climate Dynamics on December 2nd, 2021.
See the published version at https://doi.org/10.1007/s00382-021-06071-6.

Future Trends of Arctic Surface Wind Speeds and their Relationship with Sea Ice in CMIP5 Climate Model Simulations

Stephen J. Vavrus*
Nelson Institute Center for Climatic Research
University of Wisconsin-Madison
1225 West Dayton Street
Madison, WI (USA) 53706

Ramdane Alkama
European Commission
Joint Research Centre
Ispra, Italy

* Corresponding author (sjvavrus@wisc.edu), ORCID ID: 0000-0002-7612-3109

Abstract

Recent climate change in the Arctic has been rapid and dramatic, leading to numerous physical and societal consequences. Many studies have investigated these ongoing and projected future changes across a range of climatic variables, but surprisingly little attention has been paid to wind speed, despite its known importance for sea ice motion, ocean wave heights, and coastal erosion. Here we analyzed future trends in Arctic surface wind speed and its relationship with sea ice cover among CMIP5 global climate models. There is a strong anticorrelation between climatological sea ice concentration and wind speed in the early 21st-century reference climate, and the vast majority of models simulate widespread future strengthening of surface winds over the Arctic Ocean (annual multi-model mean trend of up to 0.8 m s^{-1} or 13%). Nearly all models produce an inverse relationship between projected changes in sea ice cover and wind speed, such that grid cells with virtually total ice loss almost always experience stronger winds. Consistent with the largest regional ice losses during autumn and winter, the greatest increases in future wind speeds are expected during these two seasons, with localized strengthening up to 23%. As in other studies, stronger surface winds cannot be attributed to tighter pressure gradients but rather to some combination of weakened atmospheric stability and reduced surface roughness as the surface warms and melts. The intermodel spread of wind speed changes, as expressed by the two most contrasting model results, appears to stem from differences in the treatment of surface roughness.

Keywords: Arctic, wind, sea ice, climate change, CMIP, model

Declarations:

Funding/Acknowledgments: This research was supported by a grant from the Office of the Vice Chancellor for Research and Graduate Education at the University of Wisconsin-Madison. We would also like to acknowledge high-performance computing support from Cheyenne provided by NCAR's Computational and Information Systems Laboratory, sponsored by the National Science Foundation.

Conflicts of interest: The authors declare no conflicting interests, financial or otherwise.

Availability of data: All CMIP5 model output is publicly available from the Earth System Grid, https://esgf-node.llnl.gov/search/cmip5/.

Code availability: Not applicable

Authors' contributions: Not applicable

1. Introduction

The Arctic is undergoing a dramatic transformation in response to the warming climate, with serious societal and environmental consequences. Diminishing sea ice in particular has directly contributed to an array of major changes in the region, including greatly expanded marine access (Stevenson et al. 2019), heightened geopolitical tensions (Shea 2019), and coastal erosion severe enough to cause community relocations (Barnhart et al. 2014; Marino and Lazrus 2015). A number of studies have investigated accompanying changes in the atmospheric circulation of the Arctic, some of which may abet warming and thawing, such as cyclones, the Arctic Dipole pattern, remote teleconnections from the tropics, and atmospheric rivers (Wang et al. 2009; Vavrus 2013; Ding et al. 2014; Hegyi and Taylor 2018).

Surface winds are also an important element of high-latitude circulation, and they are closely related to cyclones and ocean wave heights. Most studies investigating Arctic wind fields have focused on cyclones (Serreze et al. 1993; Simmonds et al. 2008; Serreze and Barrett 2008; Vavrus 2013), but there are differences in the literature about how best to define Arctic cyclones (Koyama et al. 2017, Oh et al. 2020). By regulating ocean wave heights, wind velocities strongly affect coastal erosion (Overeem et al. 2011), marine navigation (Dobrynin et al. 2012), carbon cycling (Fritz et al. 2017), and sea ice cover (Zhang et al. 2013).

Despite their widespread impacts, surprisingly little attention has been paid to how surface winds respond to the warming climate and what practical effects these changes will have. For example, erosion rates are known to depend on wind velocity, shoreline permafrost, sea level, ocean heat content, and sea ice concentration, yet while the latter four factors are unequivocally changing so as to promote coastal inundation, the corresponding changes in Arctic winds are less certain. A number recent studies have shown convincing evidence of increasing surface wind speeds or wave heights over the Arctic Ocean as the region warms (Spreen et al. 2011; Stegall and Zhang 2012; Wang et al. 2015; Zhang et al. 2018; Waseda et al. 2018, Jakobson et al. 2019), and these trends are expected to continue in the future (McInnis et al. 2011; Dobrynin et al. 2012; Khon et al. 2014; Aksenov et al. 2015; Ruosteenoja et al. 2019). However, most of these prior studies were limited by focusing only on a single season or region of the Arctic, and they did not address the cause of the strengthened winds.

A few exceptions are the investigations by Mioduszewski et al. (2018), Jakobson et al. (2019), and Alkama et al. (2020). The first study used output from the Community Earth System Model's Large Ensemble (CESM-LE) (Hurrell et al. 2013; Kay et al. 2015) and reported a robust future strengthening of Arctic surface winds under greenhouse warming, especially during autumn and winter and particularly for extreme wind speeds. Mioduszewski et al. (2018) identified three causal factors: (a) the typical reduction in ocean surface roughness caused by a transition from ice-covered to open water (Wadhams 2000, Knippertz et al. 2000), (b) reduced atmospheric stability and greater vertical momentum mixing due to enhanced surface warming, and (c) a poleward shift of storm tracks and associated baroclinicity. Jakobson et al. (2019) used the NCEP CFSR Reanalysis to analyze variations and trends in surface wind speed and sea

ice during the observational record (1979-2015). They found that warming and sea ice retreat cause reductions in both atmospheric stratification and surface roughness that favor stronger surface winds. Alkama et al. (2020) applied a combination of atmospheric reanalyses and climate model output from the Coupled Model Intercomparison Phase 5 (CMIP5) to document relationships between sea ice concentration and surface wind velocity during the historical record. Their analysis revealed bidirectional causality, such that ice loss promotes stronger winds (especially poleward) and vice versa, and it suggests that future sea ice loss will foster enhanced surface winds.

This body of previous work lays the groundwork for the present study, which investigates future trends in Arctic surface wind speeds among CMIP5 models as the region warms and sea ice diminishes. Based on prior results, we expect that surface winds will become stronger as a function of ice loss. Our research centers around three underlying questions:

(1) Is the hypothesized strengthening of future Arctic winds robust among climate models?

(2) What are the seasonal and spatial variations in wind speeds and how do they relate to sea ice changes?

(3) If models do generally simulate stronger winds, then what are the physical causes? If not, then what explains the inter-model disagreement?

2. Data and Methods

For this analysis, monthly-mean surface wind speed (at 10 m height), sea level pressure, and sea ice concentration were obtained from the CMIP5 collection of global climate models (GCMs) (Taylor et al. 2011). For certain models, supplemental variables were also used for diagnosis (temperature at the surface and 850 hPa, and surface wind stress in the zonal and meridional directions). We used 28 climate models (one ensemble member each) provided by 17 international modeling centers (Table 1). The models were driven by projected radiative heating in their "future" simulations covering 2006-2100 using the strong Representative Concentration Pathway 8.5 (RCP8.5) radiative forcing. The wind and sea ice output was bilinearly interpolated to a common 2^{o} x 2.5^{o} latitude x longitude grid to allow comparison among models, whose horizontal resolution ranges from as high as 0.75^{o} x 0.75^{o} to as coarse as 3.75^{o} x 3.75^{o}. In this paper, we define seasons as follows: winter = December-February, spring = March-May, summer = June-August, and autumn = September-November. Linear trends, correlations, regressions, and inter-model agreement were used to diagnose simulated future trends on an annual and seasonal basis.

3. Results

3.1 Recent conditions

To place the future responses into context, we first present the multi-model mean climatological patterns of Arctic surface wind speed and sea ice concentration for annual-average conditions during the reference period, taken to be the first decade of the CMIP5 future simulations (2006-2015). Surface winds are almost uniformly weaker over mid-high latitude land (40°-90°N) than over ocean regions (Fig. 1a), ranging from a terrestrial minimum of 3 m s^{-1} to a marine maximum of 9 m s^{-1}. The overall pattern and magnitude of wind speeds simulated by the CMIP5 models is realistic, compared with those from NCEP-NCAR Reanalysis (Mioduszewski et al. 2018). Of particular relevance for this study is the strikingly distinct difference between generally strong winds over the open ocean and weaker winds where sea ice is common (Fig. 1b) and high surface pressure is prevalent. In fact, the lightest wind speeds over the Arctic Ocean are collocated with the highest concentration of sea ice north of the Canadian Archipelago. This strongly inverse relationship between wind strength and sea ice coverage suggests that the emergence of open water as Arctic sea ice retreats in the future could coincide with increased wind speeds.

3.2 Future trends (annual)

Surface winds are simulated to strengthen noticeably through year 2100 over the Arctic Ocean and adjacent seas, including Hudson Bay. Widespread increases of 0.5 m s^{-1} or more (10%+) in the mean annual wind speed are common across the Arctic Ocean (Fig. 2a,b), and the positive trend is very robust among the vast majority of GCMs (Fig. 2d). In sharp contrast to this marine-based signal, surface winds over adjacent lands generally weaken or display no clear trend, either in the sign of change or inter-model agreement. We assess statistical significance in terms of robustness in the sign of the wind speed change across GCMs. Purely random trends among the 28 models would produce a 4.4% likelihood of 19 or more GCMs (68% of all models) agreeing on a positive trend or a negative trend. We therefore use these bounds as a measure of significance by masking out in gray where intermodal agreement is greater than 32% and less than 68% (Fig. 2d). Compared with a conventional approach of computing the statistical significance based on the multi-model average, our method has the advantage of upweighting the most commonly simulated patterns and downweighting outlier features, such as the prominent wind reduction over northeast Siberia (Figs. 2a,b) that occurs in only two closely related models (MIROC-ESM and MIROC-ESM-CHEM).

The sign of the local change in wind speed closely conforms to the presence of sea ice, whose coverage declines everywhere (Fig. 2c), such that surface winds typically strengthen where sufficient ice cover exists in the early 21st century, regardless of the magnitude of future ice loss. In fact, among grid cells considered sea ice-covered during the reference period (at least 0.15 annual-mean concentration), 95% experience a positive future trend in surface wind speed. By contrast, winds over consistently open ocean are projected to weaken virtually everywhere, with the largest reductions south of Greenland that are simulated robustly across models. The direct relationship between sea ice coverage and wind speed can even be detected at small scales, as shown by the collocation of greatest wind strengthening and ice loss around Franz Josef Land on one side of the Arctic Ocean and over the Chukchi and East Siberian Seas on the other.

The overall spatial pattern of projected wind changes and its relationship with sea ice can be expressed both in terms of the multi-model mean shown in Fig. 2 and also decomposed by model and summarized over all grid cells experiencing a (negative) sea ice trend from 2006-2100. The spatial correlation coefficient between the multi-model mean trends in wind speed and sea ice concentration over ice-covered grid cells (Fig. 2a vs. 2c) is a remarkably high -0.84. All but three of the 28 CMIP5 models simulate an inverse correlation between annual trends in surface wind speed and sea ice concentration (Fig. 3a), and the vast majority generate large negative correlations of at least -0.55 and up to -0.97. Averaged over all models, the correlation is -0.67. The three outlier models are IAP-FGOALS-s2 (r=0.11) and both MRI models (MRI-CGCM3 and MRI-ESM1, r=0.76 and 0.75 respectively), while CSIRO-Mk3.6 produces only a slightly negative correlation. GCM resolution plays no significant role in explaining the relationship between trends in wind speed and ice concentration (r = -0.28 between horizontal resolution and the model correlations shown in Fig. 3a).

The magnitude of the surface wind-sea ice relationship can be further expressed by the regression of the trends (Fig. 3b), which strongly resembles the linear correlation. Among the 24 models showing a pronounced negative correlation between trends in wind speed and ice concentration, there is a fairly large range of negative regression values but all are at least -0.51 m s^{-1} and one model (CanESM2) simulates an exceptionally strong -2.69 m s^{-1}. By contrast, both MRI models are conspicuous in generating almost equal and opposite positive regressions around 2.4 m s^{-1}. Averaged over all models, the regression is -1.13 m s^{-1}.

An interesting feature of the four most outlier models identified above is that their climatological wind speeds areally averaged over sea ice points during the reference period (2006-2015) are also unusual, as shown by the overlain red dots in Fig. 3b. In particular, the MRI models simulate very strong surface winds during the reference period of about 9.4 m s^{-1}, whereas no other CMIP5 model exceeds 6.24 m s^{-1}. Curiously, the other two outlier GCMs occupy the opposite end of the spectrum, yielding the lowest base-state wind speeds over sea ice of just 4.79 m s^{-1} (CSIRO-Mk3.6) and 3.64 m s^{-1} (IAP-FGOALS-s2). The potential role of initial wind conditions and a more in-depth analysis of the two MRI models is presented in Section 3.4.

As illustrated in Fig. 3c for all grid cells with sea ice among all models, the tendency for stronger winds with reduced sea ice coverage becomes very pronounced (almost 100% likely) when the ice decline becomes nearly complete. Furthermore, at least 90% of grid cells experience higher wind speeds if their future ice concentration shrinks by half or more. Only where very modest ice concentration occurs (< 10% trend) is the expected strengthening of overlying winds not substantial.

3.3 Future trends (seasonal)

Expected future trends in surface wind speed by season are qualitatively similar to the mean-annual projections described above, both in absolute and relative terms (Figs. 4, 5). The

greatest increases over high-latitude oceans occur during winter and secondarily autumn, while the spring and summer changes are more weakly positive. The patterns of strengthening during winter and spring largely account for the mean-annual pattern (Fig. 2a), in particular the three local regional maxima around Chukchi-East Siberian Seas, Franz Josef Land, and Hudson Bay. The highest seasonal wind increase of 1.5 m s^{-1} (23%) is located north of Wrangel Island during winter, and this localized peak affects the coastlines of northeastern Siberia and Alaska, consistent with regional climate model projections of extreme wintertime winds for Utqiagvik (Barrow) reported by Redilla et al. (2019). In addition, widespread strengthening of time-averaged wind speeds of at least 15% prevails over much of the Arctic Ocean in that season. Spatial variations are less pronounced during summer and autumn, but the pattern of stronger winds is highly coherent in both seasons and substantial during autumn, when the increase is 15% or more across most of the Arctic Ocean.

In addition, these marine-based seasonal wind trends are highly robust across GCMs, as expressed by the intermodel agreement in the sign of future changes (Fig. 6). Extremely high consistency of over 90% is seen over the entire Arctic Ocean, Baffin Bay, Hudson Bay, and western Greenland Sea for winter, and similarly strong agreement is evident over the Arctic Ocean for autumn. By contrast, most of the projected wind trends over mid-high land during these seasons are not significant. Although the magnitude of simulated future wind increases is smaller during spring and summer, there is still widespread model agreement (> 70%) over most of the Arctic Ocean, as well as high consistency for spring over Hudson Bay and the Sea of Okhotsk.

In keeping with the mean-annual conditions, the seasonal wind speed trends also show a very clear relationship with projected sea ice decline (Fig. 7). The seasonal relationships are apparent in terms of both the magnitudes and spatial patterns of the sea ice loss, such as the location of the three regional maxima described above and the more uniform changes in both wind speed and ice concentration during summer and autumn. The spatial correlation coefficients of the multi-model mean trends in wind speeds versus sea ice concentration over ice-covered grid cells vary from -0.48 (winter), -0.59 (spring), -0.63 (summer), and -0.85 (autumn).

In line with the striking sea ice-dependence is the general absence of wind strengthening over the open ocean. This tendency is especially noticeable and consistent in the North Atlantic, where winds almost uniformly weaken at all times of the year, consistent with the findings for geostrophic wind changes (Ruosteenoja et al. 2020). In most seasons and locations (especially winter), a sharp transition in sign occurs along the reference-state sea ice margin, such that stronger winds arise where ice loss occurs but weaker winds develop on the other side of this boundary.

A more detailed understanding of the seasonal changes can be found by a breakdown of the surface wind trends at all grid cells that were sea-ice covered (>15% concentration) during the reference period (Fig. 8). Although there are differences in the distributions among seasons, a commonality is that the vast majority of locations with ice cover at the start of the simulations

experience stronger winds in the future. The percentage of positive trends ranges from a low of 91% during winter and spring to 98% during summer and autumn. Also noticeable is the broader distribution of wind speed trends in autumn and winter, the two seasons in which some grid cells exceed 14% increases (modal values of 14-16% and 12-14%, respectively). By contrast, the other seasons display tighter distributions, with spring showing the weakest signal (mode = 2-4%) and summer the narrowest distribution and the most pronounced modal value of 6-8%.

3.4 Cause(s) of future wind speed changes

Stronger simulated surface winds above regions of sea ice loss have been documented previously for the ECHAM4/OPYC3 model (Knippertz et al. 2000), Polar WRF regional model (Seo and Yang, 2013), CESM model (Mioduszewski et al. 2018), atmospheric reanalyses (Jakobson et al. 2019, Alkama et al. 2020), and CMIP5 models (Ruosteenoja et al. 2020, Alkama et al. 2020). This relationship holds for both long-term trends in the past and future, as well as for interannual variability. The physical explanation has been attributed primarily to boundary layer destabilization and reduced surface roughness and secondarily to tighter pressure gradients (geostrophic wind). Consistent with Mioduszewski et al. (2018), we find that the projected future sea level pressure (SLP) trends can only be regarded as a contributing factor to stronger surface winds. In line with many studies documenting a thermal-low response to intense boundary layer heating from sea ice loss (e. g., Deser et al. 2010, Screen et al. 2014, Gervais et al. 2016), CMIP5 models collectively simulate lower SLP in all seasons, especially autumn and winter (Fig. 9). During spring and summer the decline does not exhibit strong spatial variations, but there are regional maxima associated with a deeper and poleward-shifted Aleutian Low during winter and overall deepened SLP centered over the Arctic Ocean during autumn. Only the Aleutian Low response is associated with an overlying localized strengthening of surface winds during winter (and possibly spring), whereas the other two regions of pronounced positive wind speed trends around Franz Josef Land and Hudson Bay during winter-spring are not collocated with an enhanced drop in SLP or tightened pressure gradient. The stronger Aleutian Low has been linked to a regional loss of sea ice (Gervais et al. 2016, McKenna et al., 2017, Broadman et al. 2020).

The absence of a widespread change in geostrophic wind speed leaves the other two candidates, surface roughness and atmospheric stability, as the remaining possibilities to explain the strengthened future winds. Unfortunately, surface roughness was not archived in CMIP5, and weakened stability occurs in all models (not shown), due to intense surface heating as the ice pack diminishes. We can, however, utilize the two models simulating the most opposing responses in surface wind speed trends (largest increases in CanESM2 vs. largest decreases in MRI) for comparison to diagnose their differences and infer possible causal mechanisms (as in Alkama et al. 2020). Fig. 10 summarizes the two simulations with respect to the surface wind speed climatology (reference state) and future trend, as well as the trends in sea ice concentration, SLP, and atmospheric stability.

To explain the vastly different future wind response between CanESM2 and MRI-CGCM3---whose sister model, MRI-ESM1, produces very similar results---one clue is their highly dissimilar surface wind base-state climatology over the high Arctic. Although both models produce the weakest winds during the reference period over mid-high latitude land and strong winds over the ice-free North Atlantic and North Pacific, their simulations over the Arctic Ocean are completely at odds (Fig. 10a). While CanESM2 is in line with the CMIP5 multi-model average in representing the weakest marine-based winds over the Arctic sea ice pack (Fig. 1a), MRI-CGCM3 simulates very strong winds in this region that are equal to the wind speed maximum in the North Atlantic storm track south of Greenland. This divergent signal during the reference period is mirrored by the opposing future trends, consisting of uniformly weaker (stronger) surface winds over the Arctic Ocean and adjacent ice-covered seas in MRI-CGCM3 (CanESM2) (Fig. 10b,c). Note also the more extensive ice pack in MRI-CGCM3, whose excessive coverage extends from Labrador Sea to south of Greenland and is collocated with a local wind speed maximum during the reference period. Aside from that feature, however, the two models produce broadly similar changes in future sea ice concentration and lower SLP over sea ice-covered regions (Fig. 10d), both of which agree with the collective CMIP5 response. In addition, the two models generate similar changes toward weaker atmospheric stability that are even more pronounced in MRI-CGCM3. Based on their trends in the temperature difference between the surface and 850 hPa to capture the magnitude of the characteristic Arctic temperature inversion---as in Boe et al. (2009) and Rinke et al. (2013)---the stability weakens considerably in both models where diminishing sea ice enables intense surface heating (Fig. 10e). This inter-model agreement in the response of atmospheric stability and SLP suggests that neither enhanced turbulent momentum mixing nor uniformly tighter pressure gradients can explain the consistently weaker (stronger) wind speeds where sea ice retreats in MRI-CGCM3 (CanESM2) and thus suggests that differences in the treatment of surface roughness between the models is the cause.

This supposition is supported inferentially by a breakdown of the turbulent wind stress equation, which can be used conditionally to back out the change in sign of the drag coefficient as a proxy for the missing surface roughness output. Fortunately, some CMIP5 models did save output for the zonal and meridional wind stress (*TAUx* and *TAUy*, respectively):

$$TAUx = rho * Cd * (Ua - Us)^2$$

$$TAUy = rho * Cd * (Va - Vs)^2$$

where *rho* is the air density, *Cd* is the drag coefficient, *Ua* and *Va* are the 10-m wind zonal and meridional wind speeds, and *Us* and *Vs* are the zonal and meridional ocean surface speeds. The surface roughness is represented by the drag coefficient, whose future change in sign may be inferred from the rest of the known terms. By assuming the air density will remain approximately constant and that the wind speeds are much larger than the ocean surface speeds, the simulated changes in wind stress depend only on the unknown changes in drag coefficient and known changes in wind speeds, which are negative over diminishing sea ice points in MRI-CGCM3 and positive in CanESM2. Despite the trend toward weaker surface winds

in MRI-CGCM3, the corresponding wind stress trends are actually positive in both the zonal and meridional directions, and these wind stress maxima occur where the sea ice loss is largest (Fig. 11 top). The spatial correlations between the trends in sea ice concentration and wind stress are very high for both TAUx (r = -0.73) and TAUy (r = -0.85), and all grid cells with at least 50% sea ice loss exhibit a positive trend in zonal and meridional wind stress. The only way that wind stresses can increase where wind speeds decrease over initially ice-covered grid cells is for the drag coefficient, and thus the surface roughness, to compensate by becoming larger where sea ice transitions to open water. This unexpected response indicates that sea ice is too smooth and/or open ocean is too rough in MRI-CGCM3 and may explain the excessively strong reference-state wind speeds over ice-covered regions in this model (Fig. 10a).

Unfortunately, CanESM2 did not archive wind stress, but another model (CNRM-CM5) with a nearly identically strong inverse relationship between wind speed and sea ice concentration can be used as a proxy. CNRM-CM5 produces a weakly positive agreement between stronger future winds and higher surface wind stress over diminishing sea ice locations (Fig. 11 bottom) for both TAUx (r = -0.20) and TAUy (r = -0.45), consistent with the expectation that stronger winds lead to stronger wind stress but tempered by any change in the drag coefficient. However, this concurrence cannot be used to derive the change in surface roughness, because the positive relationship between trends in wind speed and wind stress could occur whether the drag coefficient increases, remains constant, or even decreases modestly.

4. Discussion and Conclusions

This study centered around the three research questions identified at the outset:

(1) Is the hypothesized strengthening of future Arctic winds robust among climate models?

(2) What are the seasonal and spatial variations in wind speeds and how do they relate to sea ice changes?

(3) If models do generally simulate stronger winds, then what are the physical causes? If not, then what explains the inter-model disagreement?

The results demonstrate a robust future response of stronger surface winds over initially sea-ice covered regions in the CMIP5 models, particularly over the Arctic Ocean, with only one pair of closely related GCMs exhibiting a distinctly contrarian trend toward weaker winds. We find a very strong relationship between surface wind speed and sea ice concentration, such that less sea ice implies stronger winds for both contemporary and future climates. The most pronounced seasonal increases in future wind speeds over the Arctic Ocean are expected during autumn and winter, although we also find consistent strengthening over the region in spring and summer. A rigorous explanation for the stronger winds and their intermodel variations was limited by the availability of model output, but our results are consistent with previous studies in downplaying the contribution from geostrophic wind changes and highlighting the importance of future reductions in atmospheric stability and/or surface

roughness. In particular, we find that model parameterizations leading to differences in the trend of surface roughness may be critical for explaining the sign and magnitude of future wind changes over the marine Arctic.

Our findings of strengthening surface winds as Arctic sea ice transitions to open water imply a number of societally relevant consequences. First, there is the potential for a positive feedback, because wind-driven ocean turbulence can dramatically melt sea ice, as evidenced by the rapid ice loss caused by strong winds driving upward mixing of ocean heat during the Great Cyclone of 2012 (Zhang et al. 2013). Likewise, a weakened Atlantic Meridional Overturning Circulation (AMOC) promotes an expanded ice pack, which favors greater atmospheric stability and thus lighter winds and additional ice expansion (Sherriff-Tadano and Abe-Ouchi 2020). Second, stronger winds, higher ocean waves, and more open water may be offsetting factors that counter the otherwise increasingly favorable conditions for marine navigation in and around the Arctic Ocean. Third, this study has direct relevance for coastal erosion, which is already a severe and growing problem for coastal communities in the Arctic. Several known contributors to coastal erosion are expected to intensify as the region warms---diminishing coastal fast ice, higher ocean heat content, longer open-water fetch, thawing shoreline permafrost, and a rising sea level (Overeem et al. 2011, Barnhart et al. 2014)---and our results suggest that stronger surface winds should be added as an important synergistic factor.

The findings from this study also point to other conditions that will likely enhance the impacts of stronger surface winds. CMIP5 models project that the largest increases in wind speed will occur during autumn and winter, the seasons with the strongest climatological winds and regional sea ice loss. In addition, changes in the significant ocean wave height scale quadratically with changes in surface wind speed for open-water conditions without considering differences in fetch (Aksenov et al. 2015, Waseda et al. 2018). Therefore, the projected percentage increases in wind speed should lead to a squared percentage rise in significant wave heights, *even disregarding the impact of the change from a buffering ice pack to open ocean and the impact of a lengthened wind fetch as the ice pack retreats*. So a very conservative estimate, based on the modal values of seasonal wind changes noted above, is that the simulated wind strengthening will cause significant wave heights to increase by 6% in spring, 14% in summer, 28% in winter, and 32% in autumn. Accordingly, the maximum local wind increase of 23% during winter would translate to a very large 51% rise in significant wave height. Yet even these estimates are based on *monthly mean* changes in winds and do not consider the additional amplifying effect of extreme wind speeds, which at least one of the GCMs analyzed here (NCAR-CESM1-CAM5) simulates to increase over the Arctic Ocean at an even greater rate (Mioduszewski et al. 2018).

Despite the overall robust signals from CMIP5 models described here, there are several caveats to keep in mind. Future wind speeds across the marine Arctic are sensitive to the surface roughness of both sea ice and open water, and models differ considerably in how they parameterize these quantities, particularly for ice cover. Even observed values of sea ice surface roughness vary greatly as a function of ice conditions (concentration, thickness, ridging, etc.), and a warming Arctic should induce such changes even where the ice pack remains.

Furthermore, although the vast majority of GCMs simulate qualitatively similar future responses of surface wind speed and how it interacts with ice cover, there are still noteworthy differences in the magnitude of these processes that are likely to depend on biases in the atmosphere, ocean, and sea ice model components. Finally, unlike a pair of recent studies (Ruosteenoja et al. 2019, Alkama et al. 2020), our analysis did not consider changes in wind direction, which are important for a number of impacts, including thermal advection, ocean wave generation, and coastal erosion.

The results presented here lay the groundwork for possible follow-up research to investigate the extent and relevance of emerging changes in Arctic wind and sea ice coverage. One obvious next step is to conduct a similar analysis using the newly released CMIP6 to determine whether the same first-order behavior occurs. Another is to extend the geographic domain to the Southern Hemisphere to compare the coupled wind-sea ice response between polar regions, especially because the less confined Antarctic ice pack is highly sensitive to wind velocity (Holland and Kwok, 2012), although Alkama et al. (2020) found a similar basin-wide relationship for Antarctic sea ice. An additional important follow-up is to investigate the role of short-term extreme wind speeds and their disproportionate impact on wave generation, particularly if they increase by even more than the time-mean wind speeds. In this regard, a beneficial practical application of our work would be to use the GCM-simulated surface wind fields as inputs to other earth-system representations such as models of ocean waves, coastal erosion, and biogeochemical processes to assess the specific contribution from winds and to explore the broader implications of a warmer and windier Arctic.

Figure Captions

Fig. 1 Multi-model climatology (2006-2015) of annual (a) surface wind speed (m s^{-1}), (b) sea ice concentration (%)

Fig. 2 Multi-model future trend (2006-2100) in annual (a) surface wind speed (m s^{-1}), (b) surface wind speed (%), and (c) sea ice concentration (%). (d) Percentage of models simulating a positive future annual wind speed trend. Areas without significant inter-model agreement are masked in gray

Fig. 3 (a) Correlations and (b) regressions of future trends in surface wind speed vs. sea ice concentration in CMIP5 models. Mean wind speed over sea ice points in reference period of 2006-2015 is shown in red dots. (c) Mean-model probability of surface wind increase as a function of sea ice trend

Fig. 4 Multi-model future trend (2006-2100) in surface wind speed (m s^{-1}) during (a) winter, (b) spring, (c) summer, and (d) autumn

Fig. 5 Multi-model future trend (2006-2100) in surface wind speed (%) during (a) winter, (b) spring, (c) summer, and (d) autumn

Fig. 6 Percentage of models simulating a positive future annual wind speed trend during (a) winter, (b) spring, (c) summer, and (d) autumn. Areas without significant inter-model agreement are masked in gray

Fig. 7 Multi-model future trend (2006-2100) in sea ice concentration (%) during (a) winter, (b) spring, (c) summer, and (d) autumn

Fig. 8 Histogram of multi-model future trend (2006-2100) in surface wind speed (%) at all sea ice-covered grid cells during the reference period (2006-2015) in winter, spring, summer, and autumn

Fig. 9 Multi-model future trend (2006-2100) in sea level pressure (hPa) during (a) winter, (b) spring, (c) summer, and (d) autumn

Fig. 10 Comparison of MRI-CGCM3 and CanESM2 for annual (a) mean surface wind speed (m s^{-1}) during the 2006-2015 reference period, and future trends from 2006-2100 for (b) surface wind speed (m s^{-1}), (c) sea ice concentration, (d) sea level pressure (hPa), and (e) atmospheric stability (K)

Fig. 11 (top) MRI-CGCM3 future annual trends in (left) TAUx and (right) TAUy (Pa) shown as colors, with the trend in sea ice concentration (%) overlain. (bottom) Corresponding patterns in CNRM-CM5

References

Aksenov Y, Popova EE, Yool A, Nurser AJG, Williams TD, Bertino L, Bergh J (2017) On the future navigability of Arctic sea routes: High-resolution projections of the Arctic Ocean and sea ice. Marine Policy 75:300–317. https://doi.org/10.1016/j.marpol.2015.12.027

Alkama R, Koffi EN, Vavrus SJ, Diehl T, Francis JA, Stroeve J, Forzieri G, Vihma T, Cescatti A (2020) Wind amplifies the polar sea ice retreat. Env Res Lett 15:124022. https://doi.org/10.1088/1748-9326/abc379

Barnhart KR, Anderson RS, Overeem I, Wobus C, Clow GD, Urban FE (2014) Modeling erosion of ice-rich permafrost bluffs along the Alaskan Beaufort Sea coast. J Geophys Res Earth Surf 119:1155–1179. https://doi.org/10.1002/2013JF002845

Boe J, Hall A, Qu X (2009) Current GCMs' unrealistic negative feedback in the Arctic. J Clim 22:4682-4695. https://doi.org/10.1175/2009JCLI2885.1

Broadman E, Kaufman DS, Henderson ACG, Malmierca-Vallet I, Leng MJ, Lacey JH (2020) Coupled impacts of sea ice variability and North Pacific atmospheric circulation on Holocene hydroclimate in Arctic Alaska. Proc Nat Acad Sci. https://doi.org/10.1073/pnas.2016544117

Deser C, Tomas R, Alexander M, Lawrence D (2010) The seasonal atmospheric response to projected Arctic sea ice loss in the late 21st century. J Clim 23:333-351. https://doi.org/10.1175/2009JCLI3053.1

Ding Q, Wallace JM, Battisti DS, Steig EJ, Gallant AJE, Kim H-J, Geng L (2014) Tropical forcing of the recent rapid Arctic warming in northeastern Canada and Greenland. Nature 509:209–212. https://doi.org/10.1038/nature13260

Dobrynin M, Murawsky J, Yang S (2012), Evolution of the global wind wave climate in CMIP5 experiments. Geophys Res Lett, 39, L18606. https://doi:10.1029/2012GL052843

Fritz M, Vonk JE, Lantuit H (2017) Collapsing Arctic coastlines. Nature Clim Change 7(1):6–7. https://doi.org/10.1038/nclimate3188

Gervais M, Atallah E, Gyakum JR, Tremblay LB (2016) Arctic air masses in a warming world. J Clim 29:2359–2373. https://doi.org/10.1175/JCLI-D-15-0499.1

Hegyi BM, Taylor PC (2018) The unprecedented 2016-2017 Arctic sea ice growth season: the crucial role of atmospheric rivers and longwave fluxes. Geophys Res Lett 45:5204–5212. https://doi.org/10.1029/2017GL076717

Holland PR, Kwok R (2012) Wind-driven trends in Antarctic sea-ice drift, Nat Geosci 5:872–875. https://doi.org/10.1038/ngeo1627

Jakobson L, Vihma T, Jakobson E (2019) Relationships between sea ice concentration and wind speed over the Arctic Ocean during 1979-2015. J Clim 32:7783-7796. https://doi.org/10.1175/JCLI-D-19-0271.1

Khon VC, Mokhov II, Pogarskiy FA, Babanin A, Dethloff K, Rinke A, Matthes H (2014) Wave heights in the 21st century Arctic Ocean simulated with a regional climate model. Geophys Res Lett 41:2956–2961. doi:10.1002/2014GL059847.

Knippertz P, Ulbrich U, Speth P (2000) Changing cyclones and surface wind speeds over the North Atlantic and Europe in a transient GHG experiment. Clim Res 15:109–122. Doi: 10.3354/cr015109

Koyama T, Stroeve J, Cassano JJ, Crawford A (2017) Sea ice loss and Arctic cyclone activity from 1979 to 2014. J Clim 30:4735–4754. https://doi.org/10.1175/JCLI-D-16-0542.1

Marino E, Lazrus H (2015): Migration or forced displacement?: The complex choices of climate change and disaster migrants in Shishmaref, Alaska and Nanumea, Tuvalu. Human Organization 74:341–350. DOI:10.17730/0018-7259-74.4.341

McInnes KL, Erwin TA, Bathols JM (2011) Global climate model projected changes in 10m wind speed and direction due to anthropogenic climate change. Atmos Sci Lett 12:325–333. https://doi.org/10.1002/asl.341.

McKenna CM, Bracegirdle TJ, Shuckburgh EF, Haynes PH, Joshi MM (2018) Arctic sea ice loss in different regions leads to contrasting Northern Hemisphere impacts. Geophys Res Lett 45:945–954. https://doi.org/10.1002/2017GL076433

Mioduszewski J, Vavrus S, Wang M (2018) Diminishing Arctic sea ice promotes stronger surface winds. J Clim 31:8101–8119. https://doi.org/10.1175/JCLID-18-0109.s1

Oh S-G, Sushama L, Teufel BB (2020) Arctic precipitation and surface wind speed associated with cyclones in a changing climate. Clim Dyn 55:3067-3085. https://doi.org/10.1007/s00382-020-05425-w

Overeem I, Anderson RS, Wobus CW, Clow GD, Urban FE, Matell N (2011) Sea ice loss enhances wave action at the Arctic coast. Geophys Res Lett 38:L17503. https://doi.org/10.1029/2011GL048681

Redilla K, Pearl ST, Bienick PA, Walsh JE (2019) Wind climatology for Alaska: historical and future. Atmos Clim Sci 9:683-702.

609 Rinke A, Dethloff K, Dorn W, Handorf D, Moore JC (2013) Simulated Arctic atmospheric
610 feedbacks associated with late summer sea ice anomalies. J Geophys Res Atmos 118:7698–
611 7714. https://doi.org/10.1002/JGRD.50584

612 Ruosteenoja K, Vihma T, Venalainen A (2019) Projected changes in European and North Atlantic
613 seasonal wind climate derived from CMIP5 simulations. J Clim 32:6467-6490.
614 https://doi.org/10.1175/JCLI-D-19-0023.s1
615
616 Screen JA, Deser C, Simmonds I, Tomas R (2014) Atmospheric impacts of Arctic sea-ice loss,
617 1979-2009: separating forced change from atmospheric internal variability. Clim Dyn 43:333-
618 344. https://doi.org/10.1007/s00382-013-1830-9
619
620 Seo H, Yang J (2013) Dynamical response of the Arctic atmospheric boundary layer process to
621 uncertainties in sea-ice concentration. J Geophys Res Atmos 118:12383-12402.
622 https://doi.org/10.1002/2013JD020312
623
624 Serreze MC, Box JE, Barry RG, Walsh JE (1993) Characteristics of Arctic synoptic activity, 1952–
625 1989. Meteor Atmos Phys 51:147–164. https://doi.org/10.1007/BF01030491
626
627 Serreze MC, Barrett A (2008) The summer cyclone maximum over the central Arctic Ocean. J
628 Clim 21:1048-1065. doi:10.1175/2007JCLI1810.1
629
630 Shea N (2019) As Arctic ice melts, a new Cold War brews. National Geographic.
631 https://www.nationalgeographic.com/environment/2018/10/new-cold-war-brews-as-arctic-
632 ice-melts/
633
634 Sherriff-Tadano S, Abe-Ouchi A (2020) Roles of sea ice-surface wind feedback in maintaining the
635 Glacial Atlantic Meridional Overturning Circulation and Climate. J Clim 33:3001-3018. DOI:
636 10.1175/JCLI-D-19-0431.1
637
638 Simmonds I, Burke C, Keay K (2008) Arctic climate change as manifest in cyclone behavior. J
639 Clim 21:5777–5796. https://doi.org/10.1175/2008JCLI2366.1
640
641 Spreen G, Kwok R, Menemenlis D (2011) Trends in Arctic sea ice drift and role of wind forcing:
642 1992-2009. Geophys Res Lett 38:L19501. https://doi.org/10.1029/2011GL048970
643
644 Stegall ST, Zhang J (2012) Wind field climatology, changes, and extremes in the Chukchi–
645 Beaufort Seas and Alaska North Slope during 1979–2009. J Clim 25:8075–8089.
646 https://doi.org/10.1175/JCLI-D-11-00532.1
647
648 Stevenson TC, Davies J, Huntington HP, Sheard W (2019) An examination of trans-Arctic vessel
649 routing in the Central Arctic Ocean. Mar Policy 100:83–89.
650 https://doi.org/10.1016/j.marpol.2018.11.031
651

Taylor, K.E., R.J. Stouffer, G.A. Meehl (2012) An overview of CMIP5 and the experiment design. Bull Am Met Soc 93:485-498. doi:10.1175/BAMS-D-11-00094.1

Vavrus SJ (2013) Extreme Arctic cyclones in CMIP5 historical simulations. Geophys Res Lett 40:6208–6212. https://doi.org/10.1002/2013GL058161

Wadhams P (2000) Ice in the Ocean. Gordon and Breach Science Publishers, 351 pp.

Wang J, Zhang J, Watanabe E, Ikeda M, Mizobata K, Walsh JE, Bai X, Wu B (2009) Is the Dipole Anomaly a major driver to record lows in Arctic summer sea ice extent? Geophys Res Lett 36:L05706. https://doi.org/10.1029/2008GL036706

Wang XL, Feng Y, Swail VR, Cox A (2015) Historical changes in the Beaufort–Chukchi–Bering Seas surface winds and waves, 1971–2013. J Clim 28:7457–7469. https://doi.org/10.1175/JCLI-D-15-0190.1

Waseda T, Webb A, Sato K, Inoue J, Kohout A, Penrose B, Penrose S (2018) Correlated increase of high ocean waves and winds in the ice-free waters of the Arctic Ocean. Sci Rep: 8:4489. Doi:10.1038/s41598-018-22500-9

Zhang J, Lindsay R, Schweiger A, Steele M (2013) The impact of an intense summer cyclone on 2012 Arctic sea ice retreat. Geophys Res Lett 40:720–726. https://doi.org/10.1002/grl.50190

Zhang J, Stegall ST, Zhang X (2018) Wind–sea surface temperature–sea ice relationship in the Chukchi–Beaufort Seas during autumn. Envir Res Lett 13:034008. https://doi.org/10.1088/1748-9326/aa9adb

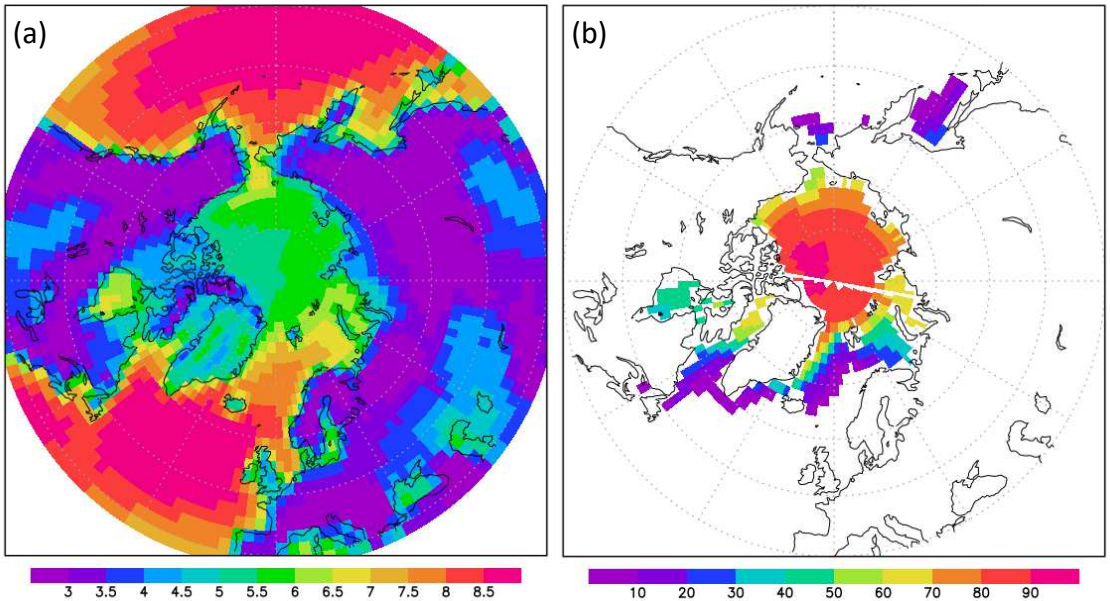

Figure 1. Multi-model climatology (2006-2015) of annual (a) surface wind speed (m s^{-1}), (b) sea ice concentration (%).

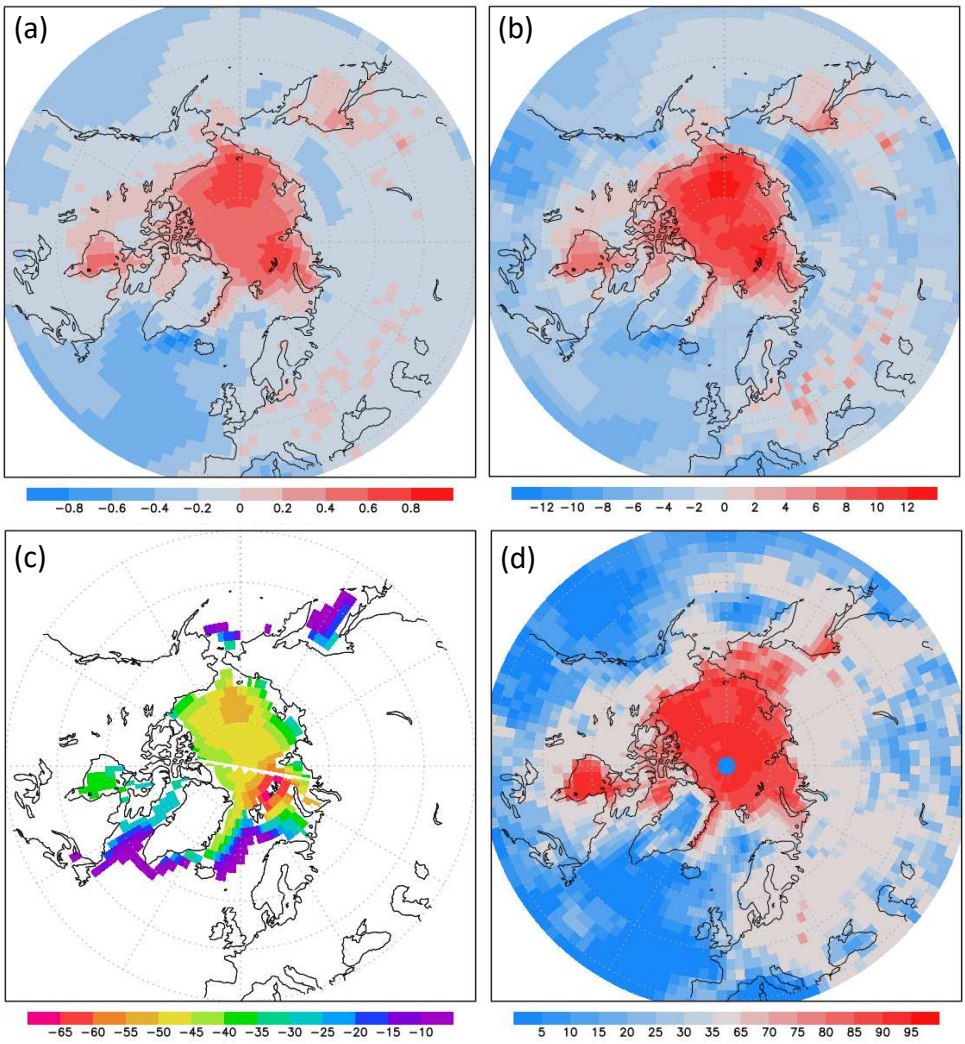

Figure 2. Multi-model future trend (2006-2100) in annual (a) surface wind speed (m s^{-1}), (b) surface wind speed (%), and (c) sea ice concentration (%). (d) Percentage of models simulating a positive future annual wind speed trend. Areas without significant inter-model agreement are masked in gray.

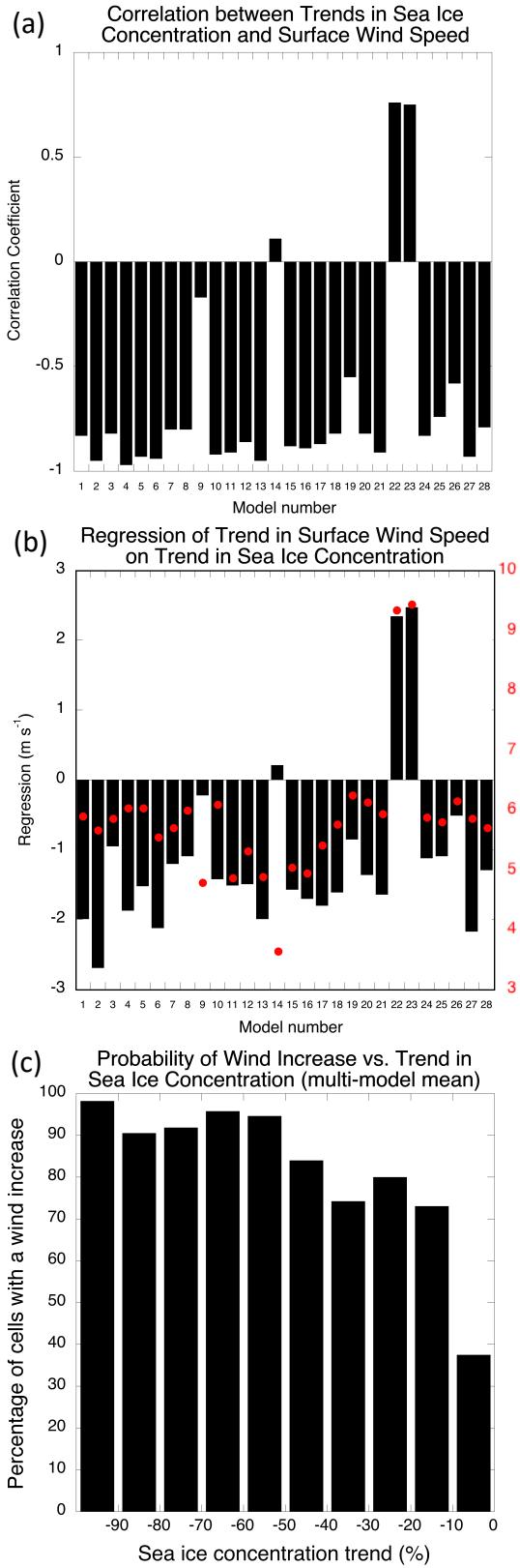

Figure 3. (a) Correlations and (b) regressions of future trends in surface wind speed vs. sea ice concentration in CMIP5 models. Mean wind speed over sea ice points in reference period of 2006-2015 is shown in red dots. (c) Mean-model probability of surface wind increase as a function of sea ice trend.

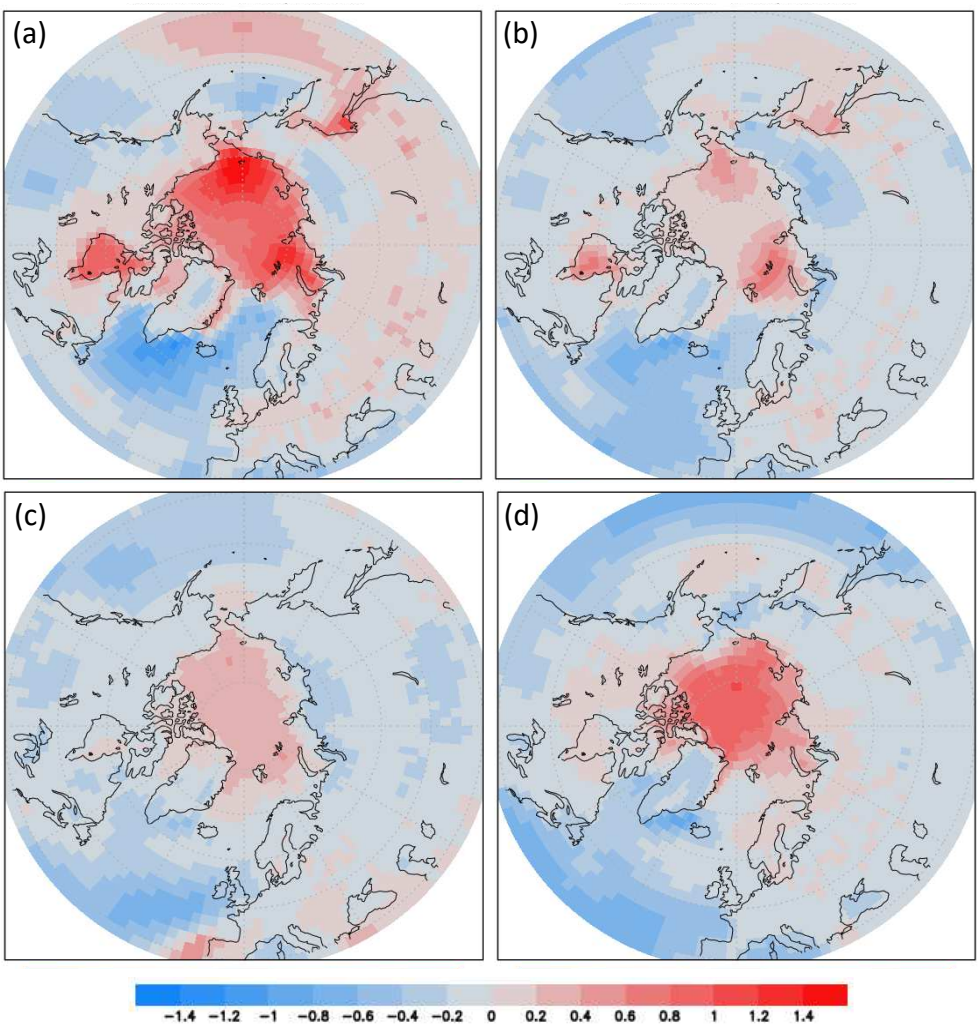

Figure 4. Multi-model future trend (2006-2100) in surface wind speed (m s^{-1}) during (a) winter, (b) spring, (c) summer, and (d) autumn.

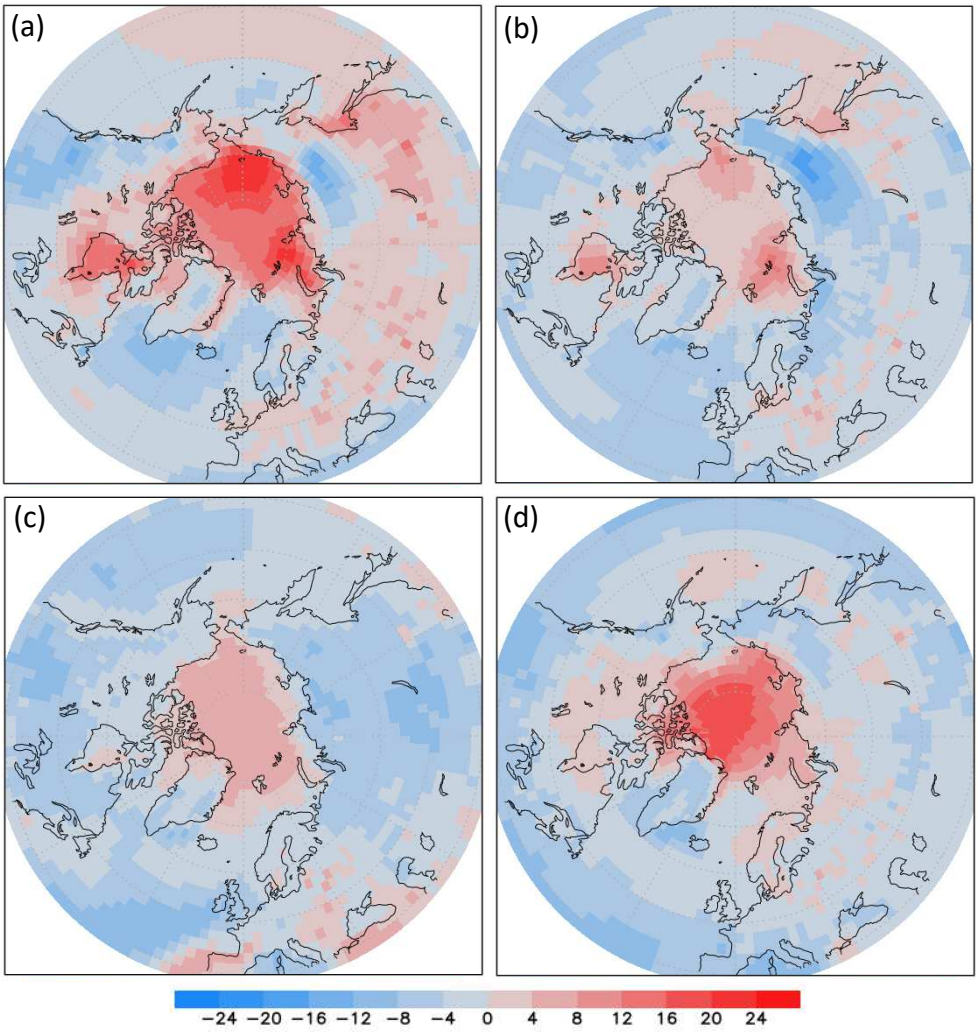

Figure 5. Multi-model future trend (2006-2100) in surface wind speed (%) during (a) winter, (b) spring, (c) summer, and (d) autumn.

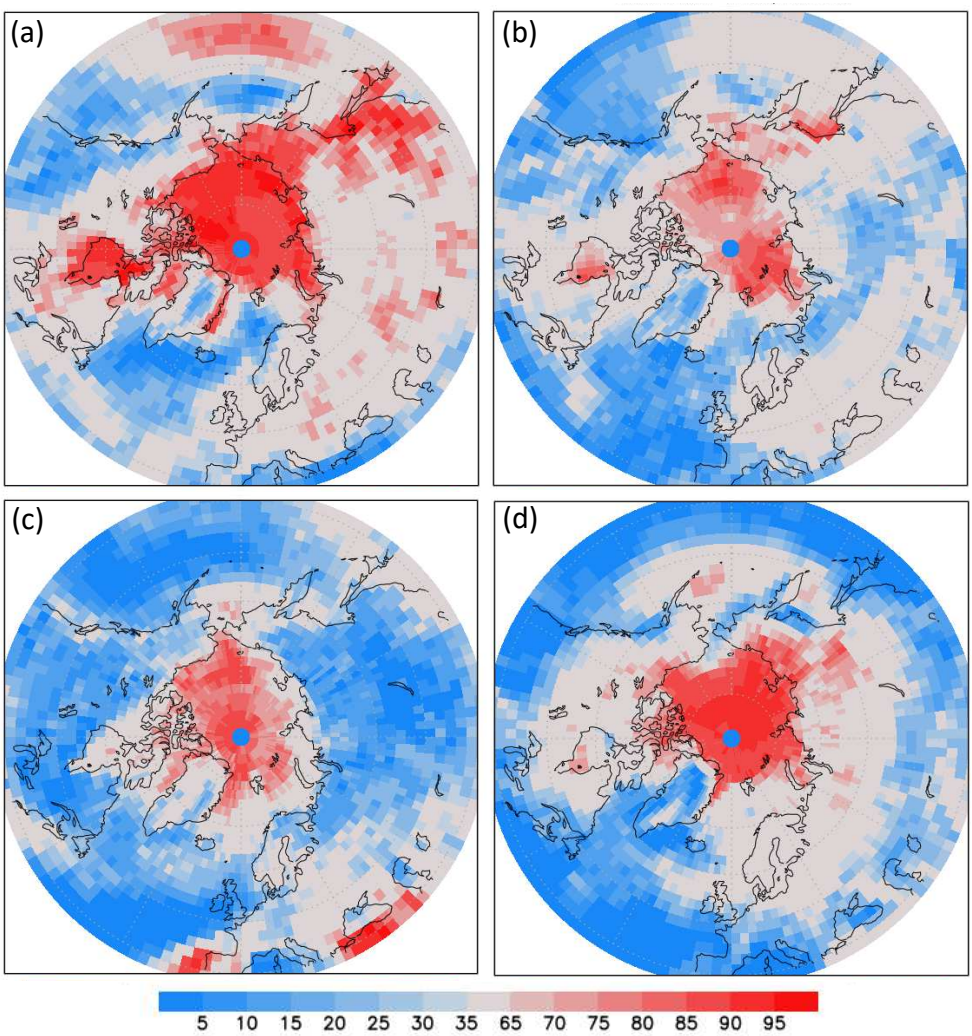

Figure 6. Percentage of models simulating a positive future annual wind speed trend during (a) winter, (b) spring, (c) summer, and (d) autumn. Areas without significant inter-model agreement are masked in gray.

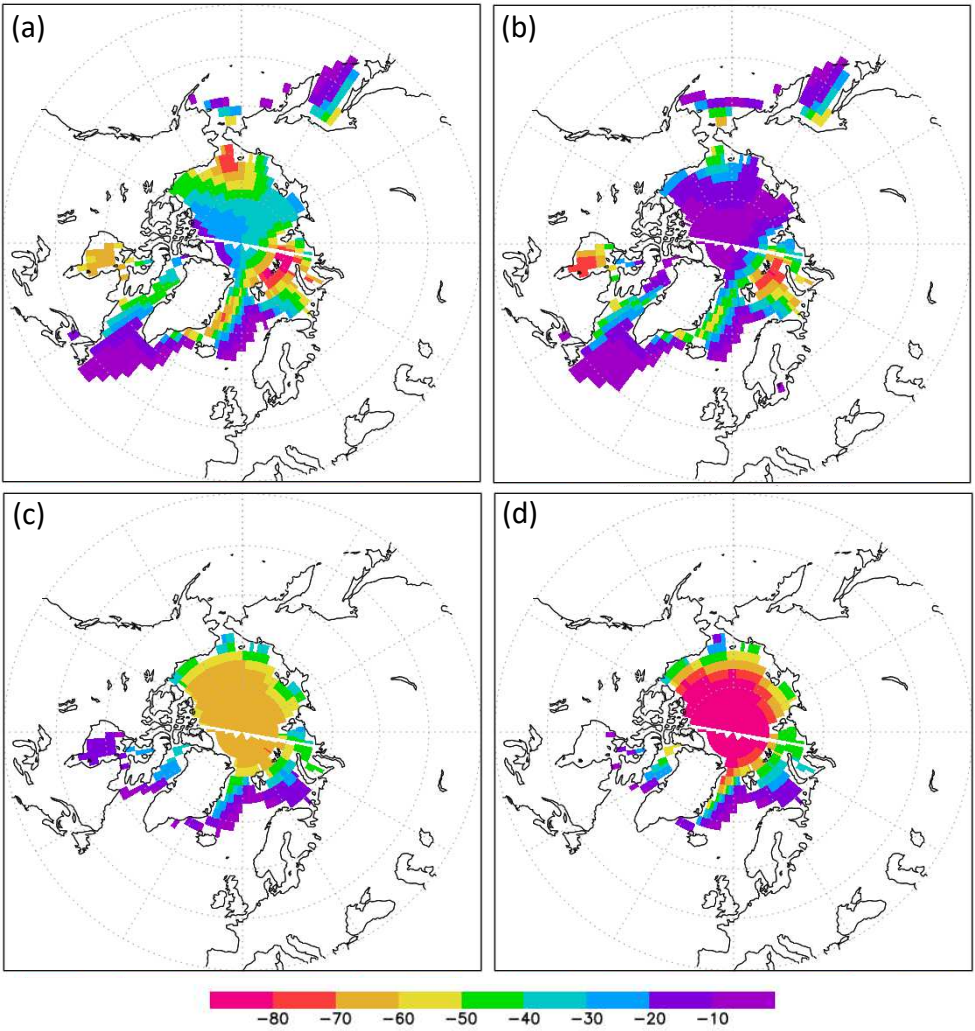

Figure 7. Multi-model future trend (2006-2100) in sea ice concentration (%) during (a) winter, (b) spring, (c) summer, and (d) autumn.

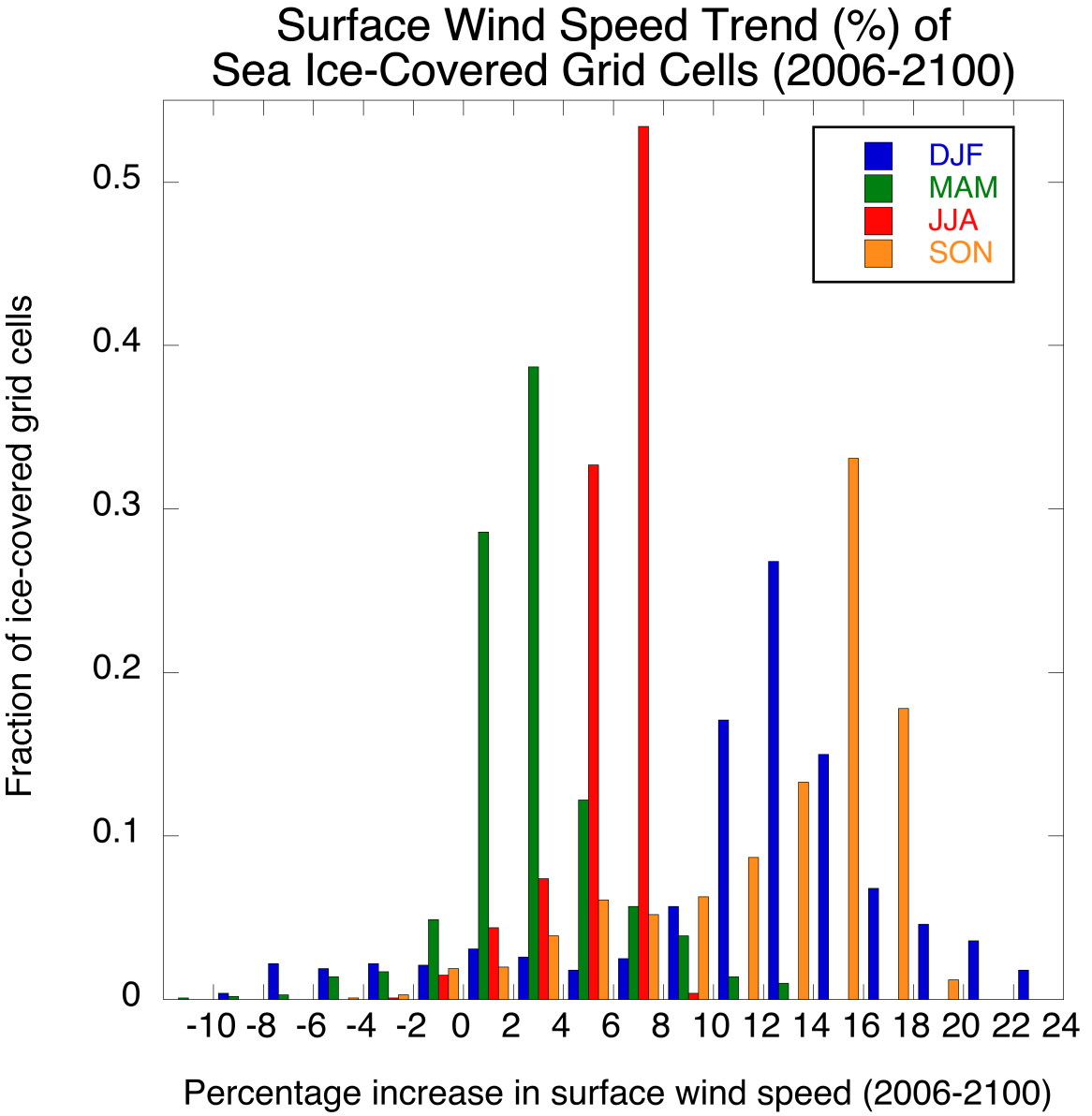

Figure 8. Histogram of multi-model future trend (2006-2100) in surface wind speed (%) at all sea ice-covered grid cells during the reference period (2006-2015) in winter, spring, summer, and autumn.

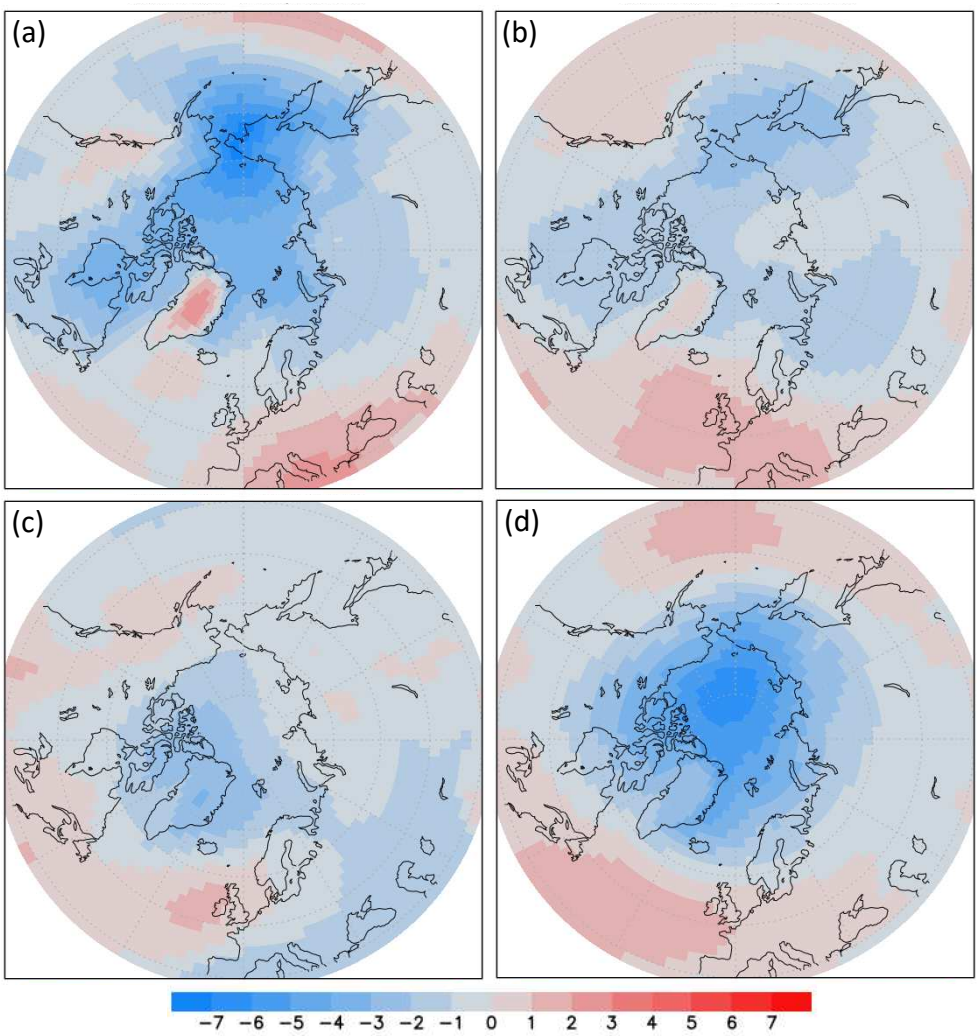

Figure 9. Multi-model future trend (2006-2100) in sea level pressure (hPa) during (a) winter, (b) spring, (c) summer, and (d) autumn.

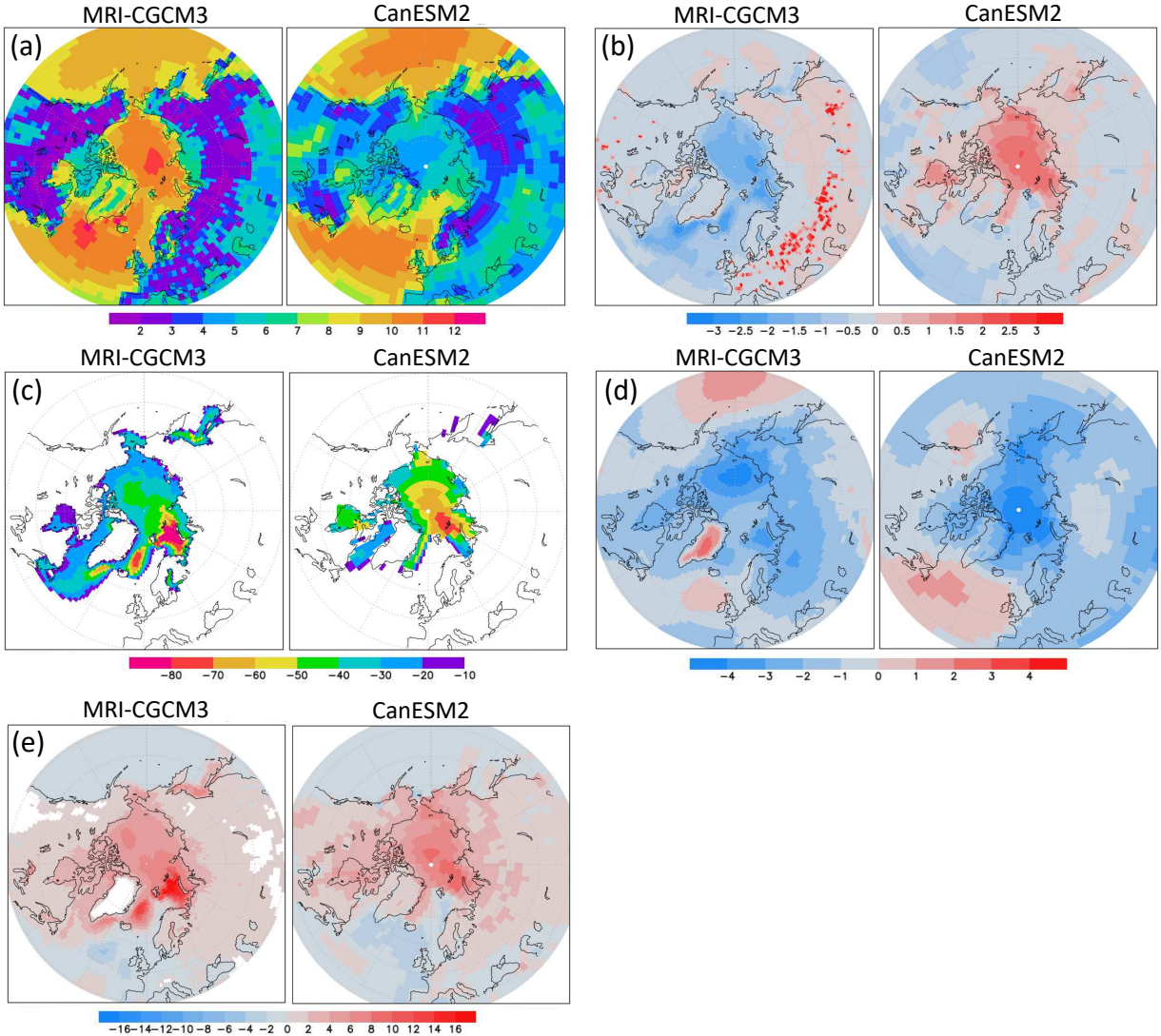

Figure 10. Comparison of MRI-CGCM3 and CanESM2 for annual (a) mean surface wind speed (m s^{-1}) during the 2006-2015 reference period, and future trends from 2006-2100 for (b) surface wind speed, (m s^{-1}), (c) sea ice concentration, (d) sea level pressure (hPa), and (e) atmospheric stability (K).

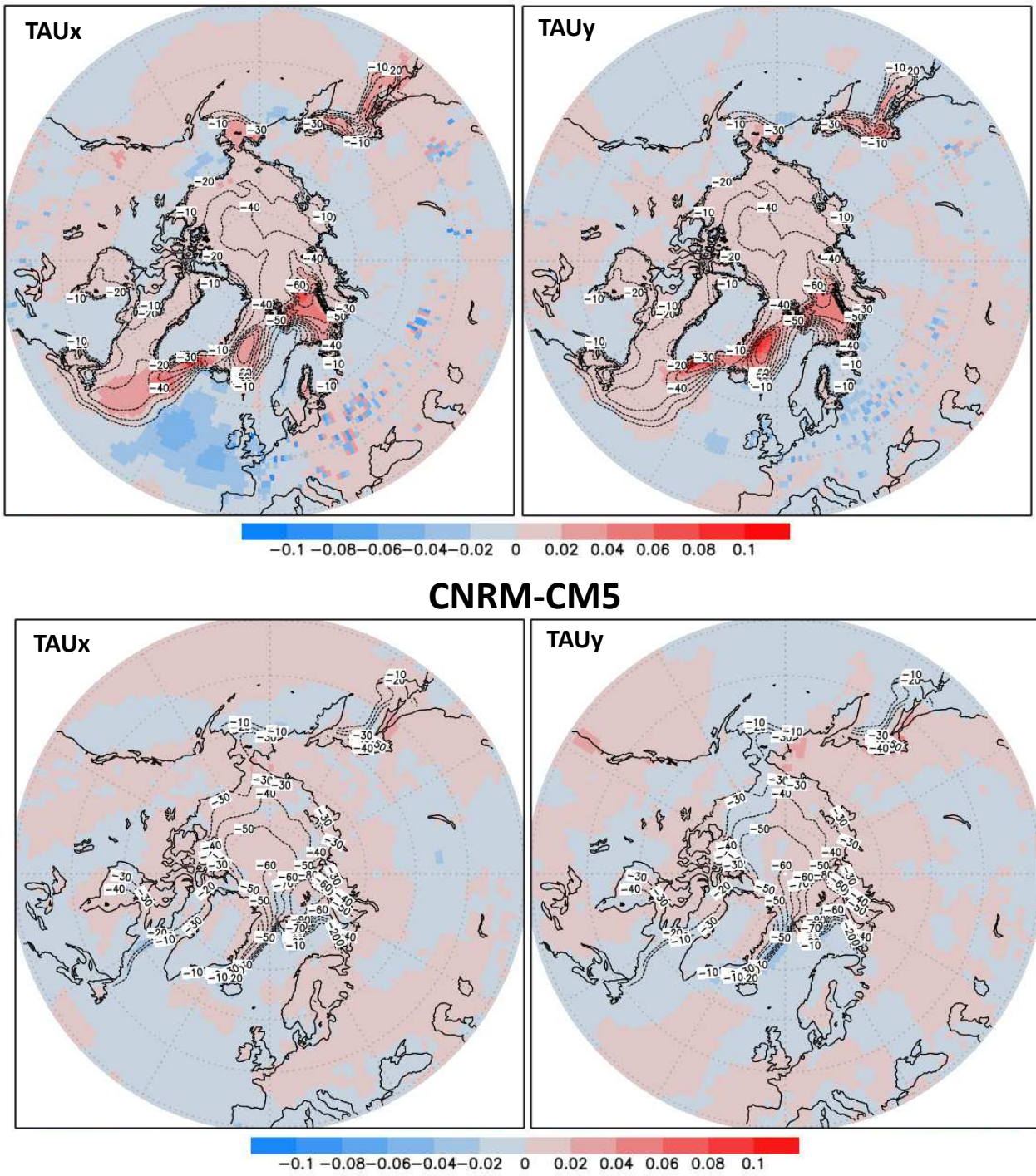

Figure 11. (top) MRI-CGCM3 future annual trends in (left) TAUx and (right) TAUy (Pa) shown as colors, with the trend in sea ice concentration (%) overlain. (bottom) Corresponding patterns in CNRM-CM5.

Table 1 Listing of the CMIP5 models used in this study. Horizontal resolution is converted into approximate degrees for the spectral models

Model	Country	Horizontal Resolution
BNU-ESM	China	2.8° x 2.8°
CanESM2	Canada	2.8° x 2.8°
CMCC-CESM	Italy	3.75° x 3.75°
CMCC-CM	Italy	0.75° x 0.75°
CMCC-CMS	Italy	1.875° x 1.875°
CNRM-CM5	France	1.4° x 1.4°
CSIRO-ACCESS1-0	Australia	1.25° x 1.875°
CSIRO-ACCESS1-3	Australia	1.25° x 1.875°
CSIRO-MK3.6	Australia	1.875° x 1.875°
ICHEC-EC-EARTH	Ireland	1.125° x 1.125°
IPSL-CM5A-LR	France	1.875° x 3.75°
IPSL-CM5A-MR	France	1.25° x 2.5°
IPSL-CM5B-LR	France	1.875° x 3.75°
IAP-FGOALS-s2	China	1.67° x 2.8°
MIROC-ESM	Japan	2.8° x 2.8°
MIROC-ESM-CHEM	Japan	2.8° x 2.8°
MIROC-MIROC5	Japan	1.4° x 1.4°
MOHC-HadGEM2-CC	United Kingdom	1.25° x 1.875°
NIMR-KMA-HadGEM2-AO	South Korea	1.25° x 1.875°
MPI-ESM-LR	Germany	1.875° x 1.875°
MPI-ESM-MR	Germany	1.875° x 1.875°
MRI-CGCM3	Japan	1.125° x 1.125°
MRI-ESM1	Japan	1.125° x 1.125°
NASA-GISS-E2-H	United States	2.0° x 2.5°
NASA-GISS-E2-R	United States	2.0° x 2.5°
NOAA-GFDL-CM3	United States	2.0° x 2.5°
NCAR-CESM1-CAM5	United States	0.9375° x 1.25°
INM-INMCM4	Russia	1.5° x 2.0°